Landscape Ecol
DOI 10.1007/s10980-013-9979-5

RESEARCH ARTICLE

Predictive modeling of spatial patterns of soil nutrients related to fertility islands

Erika L. Mudrak · Jennifer L. Schafer · Andres Fuentes-Ramirez · Claus Holzapfel · Kirk A. Moloney

Received: 11 June 2013 / Accepted: 28 December 2013

Abstract In arid shrublands, soil resources are patchily distributed around shrub canopies, forming well-studied "islands of fertility." While soil nutrient patterns have previously been characterized quantitatively, we develop a *predictive* model that explicitly considers the distance from shrubs of varying canopy sizes. In 1-ha macroplots in both the Sonoran and Mojave Deserts, we used Plant Root Simulator™ probes to measure nutrient availability along transects extending north and south from creosote bushes (*Larrea tridentata*). We modeled the decline of nutrients with distance from focal shrubs using hierarchical mixed models that included the effects of transect direction and shrub canopy size. Of the nutrients considered, nitrogen and potassium had the strongest response to distance from focal shrubs. In the Sonora, both depended on canopy size and had different patterns to the north versus the south. In the Mojave, potassium depended on size and direction, but nitrogen only on canopy size. We used the fitted model equations and the location and canopy size of all *Larrea* shrubs within the macroplots to estimate nutrient concentrations at a 20 cm resolution. This produced maps showing nutrient "hotspots" centered on *Larrea*. Our models predicted up to 60 % of the variation in nutrient availability the following growing season. Our models efficiently used a moderate number of sample locations to predict nutrient concentrations over a large area, given easily measured values of shrub size and location. Our method can be applied to many systems with patchily distributed resources focused around major structural landscape features.

Keywords *Larrea tridentata* · Ecosystem engineer · Military installation · Plant root simulator probes · Spatially explicit modeling · Nutrient hot spots

Electronic supplementary material The online version of this article (doi:10.1007/s10980-013-9979-5) contains supplementary material, which is available to authorized users.

E. L. Mudrak (✉) · A. Fuentes-Ramirez · K. A. Moloney
Department of Ecology, Evolution and Organismal Biology, Iowa State University, 251 Bessey Hall, Ames, IA 50011, USA
e-mail: mudrak@iastate.edu

J. L. Schafer · C. Holzapfel
Department of Biological Sciences, Rutgers, The State University of New Jersey, 206 Boyden Hall, Newark, NJ 07102, USA

Present Address:
J. L. Schafer
Department of Plant & Microbial Biology, North Carolina State University, 2115 Gardner Hall, Box 7612, Raleigh, NC 27695, USA

Introduction

Ecosystem engineers create or modify habitats by modulating availability of resources to other species

Published online: 08 January 2014

(Jones et al. 1994) and, in many cases, cause these resources to be patchily distributed (Rietkerk et al. 2004; Gutierrez and Jones 2006; Wright and Jones 2006). Examples of major landscape features created by ecosystem engineers that contribute to heterogeneity of soil resources include sedge tussocks, gopher mounds, and muskrat litter mounds (Gutierrez and Jones 2006). These features are found frequently in association with sessile organisms living in ecosystems with harsh physical conditions, and create positive interspecific interactions with neighboring organisms by ameliorating these conditions (Bertness and Callaway 1994). A well-studied example in arid regions is the concept of "islands of fertility" associated with perennial shrubs, which influence local soil nutrients via both physical and biotic mechanisms (e.g. Garcia-Moya and McKell 1970; Charley and West 1975; Schlesinger et al. 1996; Schade and Hobbie 2005). The resulting spatial heterogeneity of nutrients directly affects species composition and shrubs have both positive (facilitative) and negative (competitive) interactions within the native and non-native annual plant community (e.g. Holzapfel and Mahall 1999; Brooks 2003; Esque et al. 2010).

While many studies have sought to characterize soil nutrient patterns related to desert shrubs, analytical approaches vary; nonetheless, few studies incorporate an explicit consideration of shrub landscape position or canopy size and shape (but see Wilson and Thompson 2005; Butterfield and Briggs 2009; Abella et al. 2011). Canopy size and shape can affect the accumulating litter layer by influencing aerodynamics (Muller 1953). Soils under inverted-cone shaped shrubs (which have smaller basal-areas) tend to develop smaller fertility islands and have lower total soil nitrogen and carbon than shrubs with hemispherical canopies (Whitford et al. 1996; DeSoyza et al. 1997). In the northern hemisphere, shrubs cast shade to the north, creating an uneven degree of shelter for annual plants (e.g. Forseth et al. 2001; Schenk and Mahall 2002), which can result in an asymmetrical fertility island (e.g. Brooks 1998).

Most research establishes the existence of fertility islands by comparing soil from under shrub canopies with soil from the open interspace (e.g. Charley and West 1975; Schade and Hobbie 2005; Butterfield and Briggs 2009). Other studies have collected three or more soil samples at fixed distances from shrubs (Ewing et al. 2007) or at distances based on canopy size, generally employing categorical analyses (i.e. ANOVA) to assess differences in soil nutrients (e.g. Garcia-Moya and McKell 1970; Qi et al. 2010). In a few cases, researchers have employed more analytically complex spatial statistics to characterize the patterns of nutrient island formation. This often involves random, stratified random, or regular samples throughout a region of interest, ignoring shrub location, size and geometry. Geostatistical tools (such as variograms) are then used to infer spatial patterns in soil properties (e.g. Schlesinger et al. 1996; Wilson and Thompson 2005). Using these techniques, Schlesinger et al. (1996) found that soil nitrogen was autocorrelated at a scale similar to the average size of shrubs, but did not take individual shrub size or location into account. Jackson and Caldwell (1993) and Li et al. (2011) interpolated values for various soil properties via kriging to show that soil properties are highly dependent on shrub location. While geostatistical models provide an excellent mechanism for exploring the statistical properties of the spatial distribution of localized variables, it is preferable to conduct sampling in a manner than can directly account for these relationships if the goal is to understand the link between the distribution of nutrients and the locations and canopy sizes of shrubs.

In this paper, we consider whether desert soil can be efficiently sampled in a way that leads to reasonable predictions of the distribution of soil fertility over a large area. Our primary goal was to design an efficient sampling structure that maximizes general predictability using a moderate number of samples. In this way we develop a better characterization of the spatial effects of the ecosystem engineers *Larrea tridentata* on soil fertility in southwestern US deserts. We then developed models that explicitly included information on both shrub location and size to predict the spatial patterns of soil nutrients in areas containing hundreds of shrubs. We used a modification of Berger and Hildenbrandt's (2000) "field of neighborhood" model for neighborhood competition and followed the suggestions of Wright and Jones (2006) for studying the spatial effect of ecosystem engineers, which allowed us to simultaneously consider variation in nutrient concentrations between fertility islands, variation between fertility islands and the interspace, and variation at spatial scales encompassing both islands and interspace. We assess our models' abilities to predict nutrient distribution using a set of validation data.

Successful models can then be applied over a broader scale than would be possible using direct sampling techniques in the field. The approach is also applicable to other systems where the distribution of soil nutrients is controlled by patchily distributed landscape features.

Methods

Site description

We conducted our study in shrublands dominated by *Larrea tridentata* (DC) Cov. (hereafter *Larrea*) in the Sonoran and Mojave Deserts. The Sonoran Desert site (32.697°N, 112.839°W), was located at an elevation of 322 m, on a flat area within the eastern section of the Barry M. Goldwater Range, approximately 30 km south of Gila Bend, Arizona. *Larrea* is the single dominant perennial shrub at this site. Soils are coarse-loamy, hyperthermic, typic haplocalcids (Natural Resources Conservation Service 2005). At the Gila Bend NOAA Cooperative station, 29 km NNW of our site, the mean annual temperature and precipitation was 23.3 °C and 179 mm, respectively, from 1981 to 2010 (Western Regional Climate Center 2012). Our Sonoran site has two wet seasons, with rainfall occurring during both the summer and winter, whereas the Mojave site (see below) has only a winter rainfall season. A weather station (WeatherHawk 232, WeatherHawk, Logan, Utah) at our study site has been recording rainfall since November 2010.

The Mojave Desert study site (35.156°N, 116.885°W) was located at an elevation of 865 m within the Fort Irwin National Training Center, north of Barstow, California, on a southeast-facing bajada with a 7.5 % grade. The study site was co-dominated by *Larrea* and *Ambrosia dumosa* (A. Gray) Payne. For this study, we chose to work with only *Larrea* because *Ambrosia* are much smaller in comparison (mean basal area 0.53 vs. 3.47 m^2 for *Larrea*), and make up only about one tenth of the total canopy volume of *Larrea* in the study area (88 vs. 797 m^3). We also arranged our sampling regime to minimize the influence of *Ambrosia* at this site, focusing on the relationships with *Larrea*, by placing transects as far from *Ambrosia* as was possible. Soils are young and intermediate aged alluvial grus (decomposed granite; Amoroso and Miller 2006). At the Goldstone Echo 2 NOAA Cooperative station, 22 km north of the site, the mean annual temperature and precipitation was 17.7 °C and 149 mm, respectively, from 1981 to 2010 (Western Regional Climate Center 2012). A majority of the precipitation falls between January and March. A weather station at our study site has been recording rainfall since September 2010.

Field methods

In September 2010, we established one 83 × 130 m^2 macroplot in each of the Sonoran and Mojave sites. Between November 2010 and January 2011, all *Larrea* shrubs within both macroplots were georeferenced using a submeter Trimble Geo-XT 2003 GPS unit. A "shrub" was defined to be the collection of stems with overlapping canopies located on a single soil mound. We applied differential correction to location and elevation data, using the nearest base provider. This resulted in a spatial accuracy of 30–50 cm. All UTM coordinates were transformed prior to analysis so that the origin of each macroplot (i.e., (x, y) = (0, 0)) was located at the SW corner.

We measured shrub geometry using a modification of methods outlined in McAuliffe et al. (2007). We visually assessed each shrub to determine the long axis, which determined all "length" measurements, and the perpendicular axis was used for "width" measurements (Fig. 1a). For each shrub, we measured (to the nearest cm) the height (H) of the tallest living stem, length (D_1) and width (D_2) of the canopy top (defined by live stems in the upper 1/3 of the canopy), length (B_1) and width (B_2) of the canopy base (defined by living and dead branches in the lower 1/3 of the canopy), and length (S_1) and width (S_2) of the area of stems emerging from the soil surface (Fig. 1a). Projected areas of the canopy top ($A_{top} = 0.25\pi D_1 D_2$), canopy base ($A_{base} = 0.25\pi B_1 B_2$), and stems ($A_{stem} = 0.25\pi S_1 S_2$) were used to calculate shrub volume ($V_{shrub} = [H/3][A_{base} + A_{top} + (A_{base} \times A_{top})^{0.5}]$), with each shrub treated as a truncated elliptical cone.

We divided each macroplot into a 3 × 6 grid (i.e.18 subplots of 21.67 × 27.67 m^2) and collected soil data from three subplots in each. Subplots were chosen using stratified random sampling, ensuring none shared the same row or column. In early 2011, six *Larrea* shrubs per subplot were chosen as foci for the collection of soil data. The shrubs were stratified among size classes based on quantiles of V_{shrub}: 12.5–37.5 % (small, S), 37.5–62.5 % (medium, M),

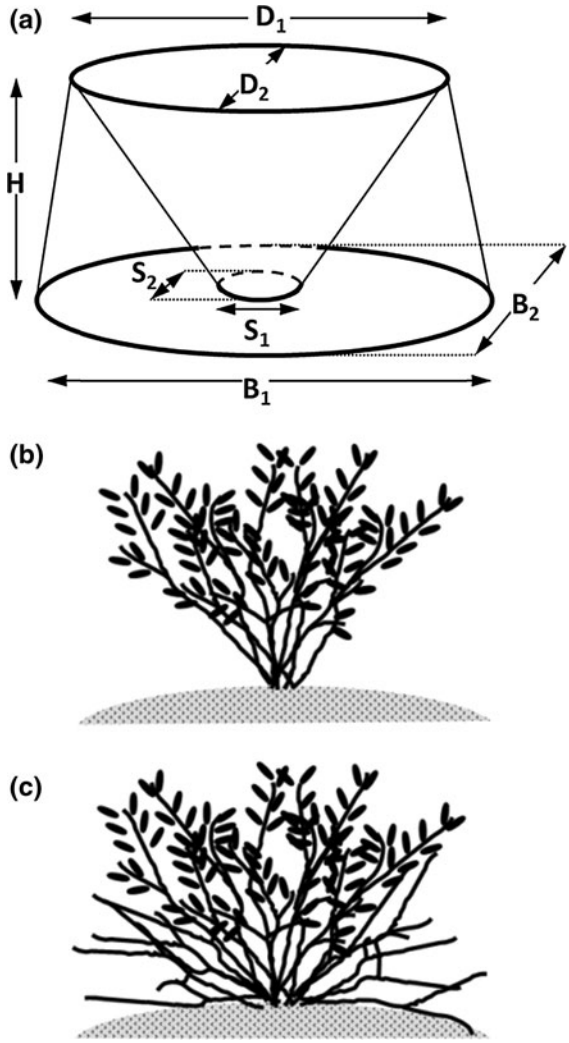

Fig. 1 **a** Measurements used to determine size of shrub canopy. See Methods for explanation of dimensions measured. **b** *Larrea* with an *inverted cone shape*. **c** *Larrea* with a *hemispherical shape*. Figure modified from McAuliffe et al. 2007

62.5–87.5 % (large, L). Each subplot included two shrubs in each size class, one of which was randomly assigned a south facing transect and the other a north facing transect. In the Mojave, transects were placed to be as far from any *Ambrosia* in the area as was possible. We used north and south transects to take into consideration potential asymmetries in the shape of fertility islands due to uneven shading. In this way, each size class was represented by each transect direction in each of the three subplots.

We sampled soil nutrients along each of the 18 transects in each macroplot using Plant Root Simulator^{TM}-probes (Western Ag Innovations, Inc., Saskatoon, Canada; hereafter termed PRS-probes). PRS-probes are ion-exchange resin membranes mounted in a plastic frame. They provide an index of the relative availability of nutrients by mimicking the uptake of ions by plants (Qian et al. 1992) and are effective in measuring nutrients in desert ecosystems (e.g. Drohan et al. 2005).

We placed the PRS-probes along transects starting at the outer edge of the stem cluster emerging from the soil. Transects extended away from the shrub (either north or south, depending on treatment) to a distance of 240 cm in the Sonoran site and 280 cm in the Mojave site. Transect lengths were based on an analysis of the location of shrub centers: 75 % of the area in the Sonoran and Mojave macroplots were within these respective distances of a *Larrea* shrub. We placed probes at 0 cm and at all multiples of 40 cm along each transect. Each transect also had two or three additional probes placed at odd multiples of 20 cm (i.e., 20, 60 cm, etc.), chosen from one of three different configurations. The additional probes were placed either at positions near the shrub, at intermediate transect distances, or at locations far from the shrub (see Fig. A1 in supplementary material). Each of the three configurations within a macroplot was used six times in a balanced design with respect to the other key factors, i.e., subplot, shrub size, and transect direction. The additional probes allowed us to generate nutrient maps at 20 × 20 cm^2 resolution with greater accuracy.

At each sample location, we inserted anion and cation PRS-probe pairs vertically into the ground (approximately 2–3 cm apart) at soil depths spanning 0.5–5.9 cm, ensuring contact between the ion-exchange surface and the soil. This depth was chosen because it has been shown that most of the horizontal variation in soil nutrients occurs at these depths in this ecosystem (Charley and West 1977; Whitford et al. 1997; Marion et al. 2008). In the Sonora, probes were installed January 28 and removed March 15, 2011, during which 35 mm of rain fell. In the Mojave, probes were installed January 18 and removed March 22, during which 7 mm of rain fell. Probes were sent to Western Ag Innovations for measurement of NH_4^+, NO_3^-, $H_2PO_4^-$, K^+, Ca^{2+}, and Mg^{2+}, which are reported in units of mg m^{-2} burial $period^{-1}$. We will hereafter refer to these nutrients as N (sum of NH_4^+ and NO_3^-), P, K, Ca, and Mg. Concentrations of NH_4^+ were below the detection limit

in 82 % of the Mojave samples and 100 % of the Sonoran samples, so the sum of NH_4^+ and NO_3^-, representing total plant available N, was used in all subsequent analyses. It should be noted that ion flux onto a probe is not linear over time (Drohan et al. 2005), so reported nutrient concentration values cannot be compared between samples over different burial periods. However, this is not an issue since our main interest is in the spatial patterns of soil nutrient availability for annual plant uptake, not the exact values of nutrients at any one time. We removed nutrient data for two shrubs from all Sonoran analyses, as they had significantly higher N concentrations than data associated with other shrubs, most likely due to their locations near a wash. We also removed three samples from the analysis of N (two in the Mojave and one in the Sonora), as the raw values were lower than blanks.

During 2012, we deployed a second set of PRS-probes to use in model validation. In each macroplot, we placed probes along transects associated with eight shrubs (not used in the 2011 study), stratified among four size classes (quantiles of V_{shrub}: 12.5–31.25 % (small), 31.25–50 % (medium-small), 50–68.75 % (medium-large), and 68.75–87.5 % (large)), with one north facing and one south facing transect in each size class. The 2011 results showed that the majority of the variation in nutrient levels occurred within 1.2 m (Mojave) or 1.6 m (Sonoran) of a shrub. To efficiently allocate our resources, we opted to shorten the transects (and number of samples in each) in exchange for including more shrubs in the validation part of the study. We placed probes at six positions—0, 20, 40, 60, 80 and 120 cm—with an additional probe at 160 cm on north transects in the Sonora, resulting in a total of 104 (Sonora) and 96 (Mojave) sample locations. Probes were installed on January 25 in the Sonora, and January 29 in the Mojave. Because of severe drought, we watered the PRS-probes to ensure that we could obtain data. On February 22 (Mojave) and 27 (Sonora) we added an equivalent of 12.5 mm of rain over a 20 × 20 cm area centered on the probes. We used tap water from Ft. Irwin and the Gila Bend Airforce Auxiliary Field, respectively. In March there was an additional 16 mm of natural rainfall in the Sonora and 1 mm in the Mojave. Probes were removed on March 23 (Sonora) and March 30 (Mojave) and were processed and analyzed as in 2011. The protocol for adding water in the area around the probes allowed us to measure relative differences in available nutrients currently in the soil, but did not capture the redistribution patterns that would occur from natural rainfall due to processes such as removal of dry deposition from *Larrea* canopies.

Model development and selection

We developed models to characterize the distribution of soil nutrients (N, P, K, Ca, and Mg) as a function of distance and direction from shrub, while also accounting for shrub size. We modeled each nutrient independently and used three general model forms: (1) regional trend models that did not incorporate shrubs; (2) linear models; and (3) negative exponential models. In the latter two cases, the effects of shrubs on nutrient distributions were explicitly modeled as a function of distance from shrub, transect direction (north or south), and shrub size (i.e., A_{base}, which will be referred to simply as A in subsequent equations). We used A_{base} to represent shrub size in our models because preliminary analyses indicated this measure was the most successful in model fitting, and because other studies have shown that the geometry of the shrub at the base is important in determining nutrient island patterns (DeSoyza et al. 1997; Whitford et al. 1996).

The regional trend models ignored the effect of shrub and consisted of a second order polynomial of the form:

$$\gamma_i = h + \beta_1 x_i^2 + \beta_2 x_i + \beta_3 x_i y_i + \beta_4 y_i + \beta_5 y_i^2 + \varepsilon_i \quad (1)$$

where γ_i is the nutrient concentration (in mg m^{-2} burial period^{-1}) of observation i at position (x_i, y_i) within the macroplot, and $\varepsilon_i \sim N(0, \sigma)$ is the error term. We fit these models using backwards elimination to remove non-significant variables.

We fit linear and negative exponential models as hierarchical, mixed-effects models, with shrub as a random effect, since the sampled shrubs represent a random subsample of the shrubs within a macroplot. The linear (Eq. 2) and negative exponential (Eq. 3) models took the form:

$$\gamma_{ij} = \Phi_i^m(A_i, \tau_i) \cdot d_{ij} + \Phi_i^c(A_i, \tau_i) + \varepsilon_{ij} \quad (2)$$

$$\gamma_{ij} = \Phi_i^a(A_i, \tau_i) \cdot \exp\left(-\Phi_i^b(A_i, \tau_i) \cdot d_{ij}\right) + \Phi_i^c(A_i, \tau_i) + \varepsilon_{ij} \quad (3)$$

where γ_{ij} is the nutrient concentration at transect position j for shrub i, d_{ij} is distance (in cm) of position j

from the shrub base, τ_i is a binary parameter denoting transect direction for shrub i (north: $\tau_i = 0$; south: $\tau_i = 1$), and $\varepsilon_{ij} \sim N(0, \sigma)$ is the sample-level error term. The parameters $\Phi_i^k(A_i, \tau_i)$in Eqs. 2 and 3 are functions of shrub size and transect direction for shrub i and were modeled as

$$\Phi_i^k(A_i, \tau_i) = \beta_0^k + \beta_1^k \tau_i + \beta_2^k A_i + \beta_3^k A_i \tau_i + \varepsilon_i^k \quad (4)$$

where k is the parameter being modeled and $\varepsilon_i^k \sim N(0, \sigma_k)$ is a parameter-level error term. When necessary, the negative exponential equation (Eq. 3) was log transformed on both sides to stabilize the variance and preserve the exponential decay relationship (Ritz and Streibig 2008).

We fit the hierarchical mixed-effects models using the nlme package (Pinheiro et al. 2011) in the R statistical programming environment (R Development Core Team 2012). We eliminated non-significant, fixed-effects parameters using a variant of stepwise backwards model selection. At each step in the selection procedure, we evaluated every possible random effects structure, creating many possible models with significant parameters. Final candidate models were required to have low correlation ($\rho < 0.15$) among multiple random effects to avoid over parameterization in the random-effects structure. Final candidate models also satisfied the requirement of having normally distributed, homoscedastic residuals.

We assessed the candidate models using Akaike's Information Criteria (AIC; Burnham and Anderson 2004), and also considered the ability of best-fit models to predict the spatial variation of the validation data (see below). We examined model residuals for evidence of overall spatial trends by visual inspection and through ANOVA, testing for differences in residuals among the three subplots in each macroplot. We also analyzed residuals using the geoR package in R (Ribeiro and Diggle 2001) and found no evidence of unaccounted spatial autocorrelation in any of the models.

Model application

We constructed maps of nutrient concentrations in the macroplots at 20 cm resolution for each of the five macronutrients using the spatstat package in R for manipulating images (Baddeley and Turner 2005). Maps developed from the hierarchical mixed effects models (Eqs. 2, 3) produced slightly different realizations each time they were constructed, because of the random effects involved. In constructing maps, we first initialized the landscape at all locations using random values drawn from a log-normal distribution, based on the variance structure of the nutrient data collected from the "interspace" (samples > 150 cm from the shrub stems). We then estimated the pattern of nutrient distributions using the candidate model under consideration. Model parameters were generated individually for each shrub, incorporating the A_{base} value and the appropriate parameter-level error term. We then estimated nutrient concentrations within the "range-of-influence" (*RI*) of each shrub. This ran from the outer edge of the shrub's stem base to a distance at which the model estimate dropped below the 90th percentile of the log-normal distribution for the interspace data (Fig. 2a). Nutrient values within the stem radius were set to values calculated at $d_{ij} = 0$. Locations within the RI of more than one neighboring shrub were assigned the maximum nutrient value calculated for any of the influencing shrubs. For models with parameter functions Φ_i^k dependent on directional estimates (i.e. north and south transect values differed significantly), we calculated nutrient values based on a weighted average according to the angle θ of the vector running from the shrub center to the location of the model cell being estimated as $(\phi_{i\,\text{avg}}^k = (\theta/180) \cdot \phi_{i\,\text{south}}^k + (1 - \theta/180) \cdot \phi_{i\,\text{north}}^k)$. This resulted in a map of nutrient "hotspots" centered on *Larrea* canopies (Fig. 2b).

Model validation

We used the validation data collected in 2012 to test the ability of our models to make accurate predictions. Because of the stochasticity incorporated in the random effects structures, we produced 100 model realizations for each candidate model. For each model realization, we regressed the observed nutrient concentrations on model predictions for each 2012 PRS-probe location, using simple linear regression. We then assessed the ability of the models to accurately predict nutrient concentrations using three measures: (i) the proportion of the replicate regression models that significantly explained the variance of the validation data ($P < 0.05$), (ii) the average proportion of the variance in the validation data that was explained (i.e., mean R^2 value), and (iii) the overall bias in model predictions (slope $\neq$ 1).

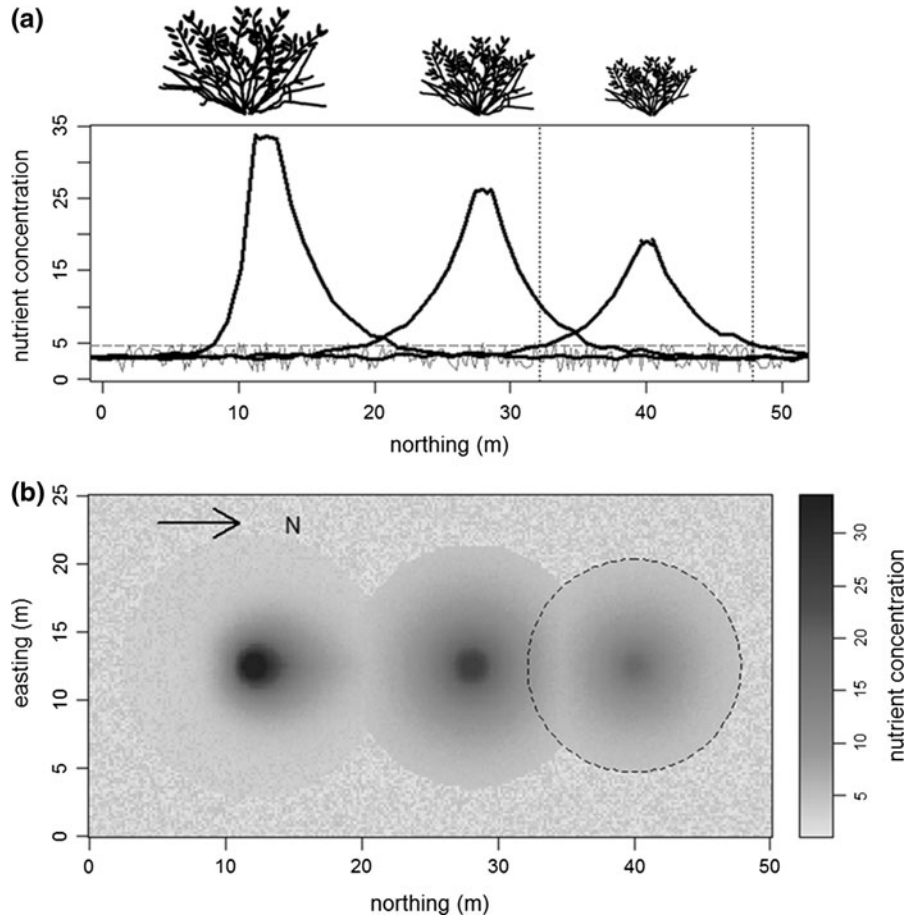

Fig. 2 Illustration of hypothetical model application using a negative exponential model. **a** Graph of individual model equations for each of three shrubs of varying size. Parameters *a* (nutrient concentration at shrub stem) and *b* (rate of decay) are positively related to shrub size, and parameter *c* is constant. The left-most shrub shows a model that includes a directional effect (unequal curves to the north and south). The *horizontal dashed line* represents the 90th percentile of values from the shrub interspace. **b** Nutrient hotspot map obtained by model curves shown in part *a*. The image is initialized with random values (background static; see text for details). The range-of-influence (*RI*) is shown for the rightmost shrub via *dotted lines*

Results

We mapped 713 *Larrea* in the Sonoran macroplot and 303 in the Mojave macroplot (Fig. 3a). In the Sonora, the average A_{base} was 2.05 m^2, and the average A_{stem} was 0.26 m^2 (Fig. 3b). In the Mojave, the shrub canopies were much larger, as the average A_{base} was 3.47 m^2 and average A_{stem} was 0.77 m^2 (Fig. 3b). In both deserts, concentrations of N and K were higher near the shrub stems and decreased with increasing distance from the shrub (Fig. 4). Concentrations of P, Ca, and Mg did not appear to be as strongly dependent on distance from the shrub stems.

Distribution of N

The best-fit model for N in the Sonora was the negative-exponential. The values obtained for the model parameters indicated that N concentrations directly under the shrub (parameter *a*) respond positively to canopy size, while the rate of decay (parameter *b*) from the shrub center to the interspace was slower on the south side of the shrub (Table 1). The *RI* values indicated that shrubs influence N concentrations up to about 0.89 m (Table 2; Fig. 5a). Overall, the model explained 60 % of the variation in the validation data, and all model simulations produced significant validation results (Table 2). The best-fit model was also very successful in predicting nutrient concentrations measured in 2012, as the slope of the regression lines were very close to the $y = x$ line (mean slope = 0.94; Table 2; Fig. 6a).

In the Mojave, the best model for N did not depend on either canopy size or transect direction (Table 1). It was successful in producing consistently significant predictions in the validation data, but never explained more than 16 % of the overall variation. Slope values were less than one (mean slope = 0.78; Table 2), with

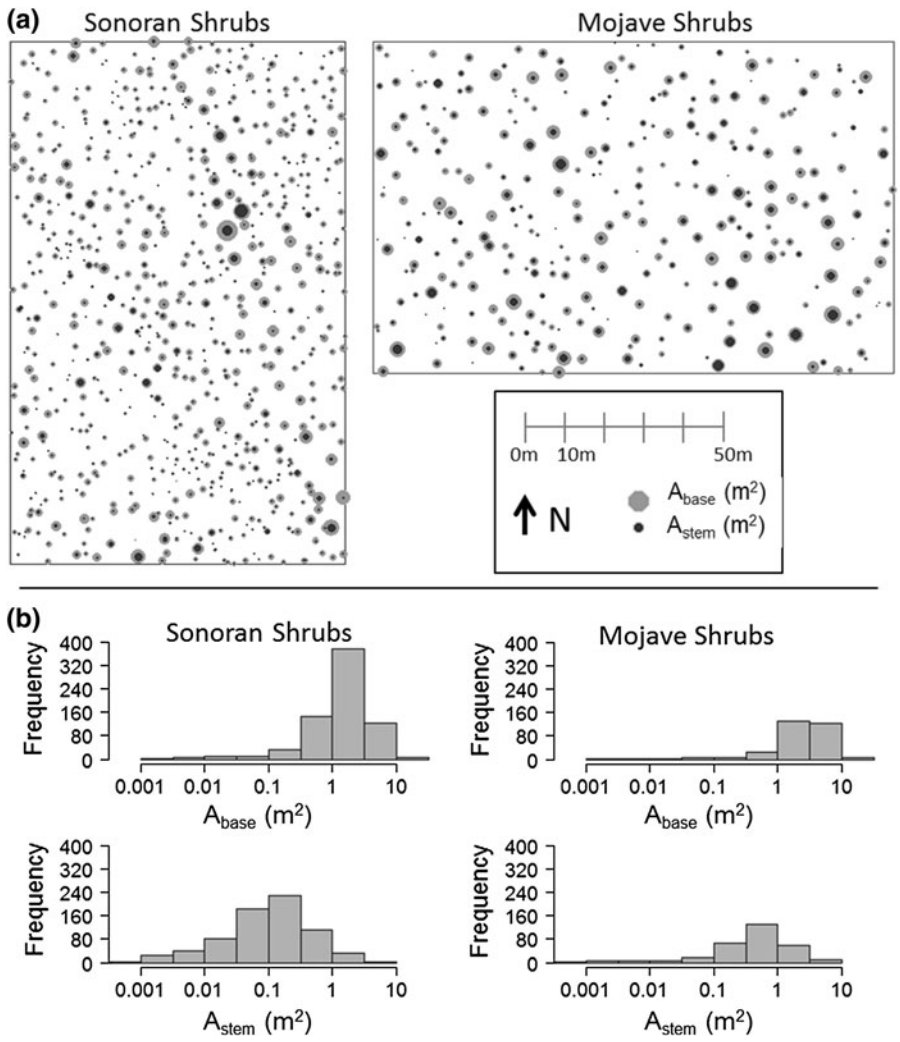

Fig. 3 **a** Maps of *Larrea* in the Sonoran and Mojave macroplots. Circular representation of A_{base} (*light gray*) and A_{stem} (*dark gray*) are shown to scale. **b** Histograms showing distributions of values for A_{base} and A_{stem} for each study site

the model underestimating low nutrient concentrations, but not high concentrations (Fig. 6b).

Distribution of P

In the Sonoran Desert, the best model for P was linear, although values for the slope (parameter *m*) were often positive, but very close to zero (<0.01 for most simulations). This result indicates a very minimal influence of shrubs on the distribution of P, resulting in an inability to predict nutrient concentrations in the validation data (8 % of simulations significant). In the Mojave, we found no evidence that P was related to distance from shrub. The best-fit regional trend model found P to vary from east to west within the macroplot (Table 1), but was not successful in predicting values for the validation data (Table 2).

Distribution of K

The best model for K in the Sonoran Desert was of the negative exponential form. Under-canopy nutrient concentration differed between the north and south sides of the shrub and the rate of nutrient decay was related to shrub canopy size (Table 1; Fig. 5c). Shrubs affected K concentrations up to approximately 1.8 m (Table 2). All simulations using this model significantly predicted K concentrations and explained, on average, 40 % of the variation in the validation data (Table 2). Average slopes of predicted values regressed on the validation data were close to one

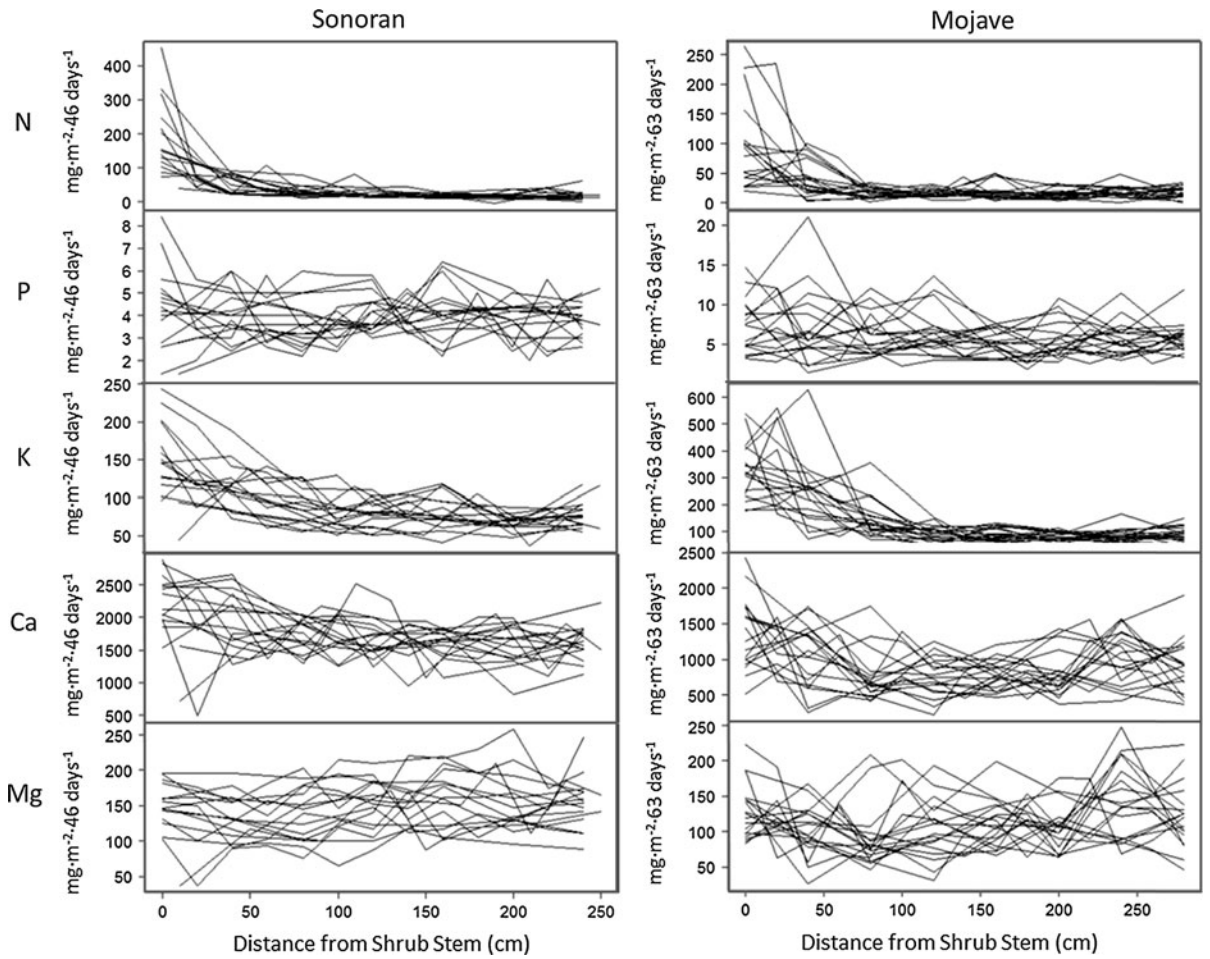

Fig. 4 Nutrient concentrations obtained from PRS-probes plotted against distance from shrub stems. *Lines* connect samples from the same transects. Note scale differences for nutrient concentrations, which are reported in mg m^{-2} burial $period^{-1}$

(mean slope = 0.93; Fig. 6c). In the Mojave, the best model for K indicated that concentrations directly under the shrub were influenced by both canopy size and direction (Table 1), with a shrub influencing concentrations to about 1.2 m (Fig. 5d). About 47 % of the variation in the validation data was explained, but the regression lines were shallow (mean slope = 0.44; Table 2), with the models tending to underestimate low nutrient concentrations and overestimate high nutrient concentrations (Fig. 6d).

Distribution of Ca and Mg

Negative exponential models provided the best fit for Ca in both deserts, indicating that distance from shrub was important, but neither size nor direction were significant factors (Table 1). The Sonoran model was moderately successful in predicting Ca concentrations from the validation data (59 % of model simulations had $P < 0.05$), but explained only 16 % of the variation. The Mojave model was not very successful in predicting Ca concentrations (only 13 % of model simulations had $P < 0.05$), explaining only 13 % of the variation in the validation data.

The best model for Mg in the Sonora was linear with the rate of change with distance from shrub (m, or slope) dependent on size (Table 1). Though this parameter was significant, slope values were low and sometimes positive when equations were evaluated for all shrubs in the macroplot. In the Mojave, the regional

Table 1 Model structure and parameter estimates for the best-fit model for each nutrient

Desert	Nutrient	Model type	Model equation(s)
Sonoran	N	Neg. exp	$\gamma_{ij} = \Phi_i^a(A_i) \cdot \exp\left(-\Phi_i^b(A_i, \tau_i) \cdot d_{ij}\right) + \Phi_i^c + \varepsilon_{ij}$
			$\Phi_i^a = 66.734 + 30.779 \cdot \mathrm{A_i}$
			$\Phi_i^b = 0.0498 - 0.0096 \cdot \tau_\mathrm{i} - 0.00376 \cdot \mathrm{A_i}$
			$\Phi_i^c = 17.897 + {}_i^c;\ \varepsilon_i^c \sim \mathrm{N}\ (0, 4.121)$
			$\varepsilon_{ij} \sim \mathrm{N}\ (0, 0.378)$
Sonoran	P	Linear	$\gamma_{ij} = \Phi_i^m(A_i) \cdot d_{ij} + \Phi_i^c(A_i) + \varepsilon_{ij}$
			$\Phi_i^m = -0.00713 + 0.00330 \cdot \mathrm{A_i}$
			$\Phi_i^c = 5.066 - 0.511 \cdot \mathrm{A_i} + \varepsilon_i^c,\ \varepsilon_i^c \sim \mathrm{N}\ (0, 0.0614)$
			$\varepsilon_{ij} \sim \mathrm{N}\ (0, 1.0482)$
Sonoran	K	Neg. exp	$\gamma_{ij} = \Phi_i^a(\tau_i) \cdot \exp\left(-\Phi_i^b(A_i) \cdot d_{ij}\right) + \Phi_i^c + \varepsilon_{ij}$
			$\Phi_i^a = 101.563 - 51.745 \cdot \tau_\mathrm{i}$
			$\Phi_i^b = 0.0216 - 0.00287 \cdot \mathrm{A_i}$
			$\Phi_i^c = 67.842 + \varepsilon_i^c;\ \varepsilon_i^c \sim \mathrm{N}\ (0, 6.016)$
			$\varepsilon_{ij} \sim \mathrm{N}\ (0, 0.225)$
Sonoran	Ca	Neg. exp	$\gamma_{ij} = \Phi_i^a \cdot \exp\left(-\Phi_i^b \cdot d_{ij}\right) + \Phi_i^c + \varepsilon_{ij}$
			$\Phi_i^a = 546.613 + \varepsilon_i^a;\ \varepsilon_i^a \sim \mathrm{N}\ (0, 374.897)$
			$\Phi_i^b = 0.0155$
			$\Phi_i^c = 1581.260$
			$\varepsilon_{ij} \sim \mathrm{N}\ (0, 316.884)$
Sonoran	Mg	Linear	$\gamma_{ij} = \Phi_i^m(A_i) \cdot d_{ij} + \Phi_i^c(A_i) + \varepsilon_{ij}$
			$\Phi_i^m = 0.130 + 0.106 \cdot \mathrm{A_i}$
			$\Phi_i^c = 181.796 - 21.841 \cdot \mathrm{A_i} + \varepsilon_i^c;\ \varepsilon_i^c \sim \mathrm{N}\ (0, 22.58)$
			$\varepsilon_{ij} \sim \mathrm{N}\ (0, 26.868)$
Mojave	N	Neg. exp	$\gamma_{ij} = \Phi_i^a \cdot \exp\left(-\Phi_i^b \cdot d_{ij}\right) + \Phi_i^c + \varepsilon_{ij}$
			$\Phi_i^a = 65.0622$
			$\Phi_i^b = 0.0395 + \varepsilon_i^b;\ \varepsilon_i^b \sim \mathrm{N}\ (0, 0.000002)$
			$\Phi_i^c = 14.0935$
			$\varepsilon_{ij} \sim \mathrm{N}\ (0, 0.655)$
Mojave	P	Regional	$\gamma_i = 6.617 - 0.016 y_i + \varepsilon_i; \varepsilon_i \sim N(0, 2.761)$
Mojave	K	Neg. exp	$\gamma_{ij} = \Phi_i^a(A_i, \tau_i) \cdot \exp\left(-\Phi_i^b \cdot d_{ij}\right) + \Phi_i^c + \varepsilon_{ij}$
			$\Phi_i^a = 144.415 + 89.059 \cdot \tau_\mathrm{i} + 28.647 \cdot \mathrm{A_i}$
			$\Phi_i^b = 0.0207 + \varepsilon_i^b;\ \varepsilon_i^b \sim \mathrm{N}\ (0, 0.00533)$
			$\Phi_i^c = 73.247$
			$\varepsilon_{ij} \sim \mathrm{N}\ (0, 0.315)$
Mojave	Ca	Neg. exp	$\gamma_{ij} = \Phi_i^a \cdot \exp\left(-\Phi_i^b \cdot d_{ij}\right) + \Phi_i^c + \varepsilon_{ij}$
			$\Phi_i^a = 529.580 + \varepsilon_i^a;\ \varepsilon_i^a \sim \mathrm{N}\ (0, 0.0585)$
			$\Phi_i^b = 0.0357$
			$\Phi_i^c = 854.0058$
			$\varepsilon_{ij} \sim \mathrm{N}\ (0, 356.816)$
Mojave	Mg	Regional	$\gamma_i = 106.7 + 0.314 y_i + \varepsilon_i; \varepsilon_i \sim N(0, 41.26)$

Nutrient concentration (in mg m^{-2} burial $period^{-1}$) is denoted as γ_i (observation i at position (x_i, y_i) for a regional model) or as γ_ij (transect position j for shrub i for negative exponential and linear models), d_{ij} is the distance (cm) of position j from shrub stems, τ_i is a binary variable denoting transect direction for shrub i (0 if north, 1 if south), and $\varepsilon_{ij} \sim \mathrm{N}\ (0, \sigma)$ is the error term at the sample level

Table 2 Validation analyses for best-fit models of five macronutrients in the Sonoran and Mojave Desert macroplots

Desert	Nutrient	Model type	Mean *RI* (m)	% runs with $P < 0.05$	Mean R^2	Mean slope of regression
Sonoran	N	Neg. exp	0.886	100	0.598	0.94
	P	Linear	2.118	8	0.124	0.19
	K	Neg. exp	1.767	100	0.400	0.93
	Ca	Neg. exp	0.759	59	0.155	0.42
	Mg	Linear	3.062	7	0.097	−0.08
Mojave	N	Neg. exp	0.983	100	0.159	0.78
	P	Regional	–	5	0.128	−0.58
	K	Neg. exp	1.209	100	0.471	0.44
	Ca	Neg. exp	0.970	13	0.128	0.42
	Mg	Regional	–	4	0.099	−0.004

RI (range of influence) indicates the distance at which the model equation drops below the 90th percentile of the interspace nutrient concentrations. Model fit was assessed by regressing observed nutrient concentrations on the estimated concentrations produced by each of the 100 model runs. We report the percent of model runs with significant regression models ($P < 0.05$). For the set of model runs with significant regressions, we report the mean R^2 value and the mean slope (see Fig. 6)

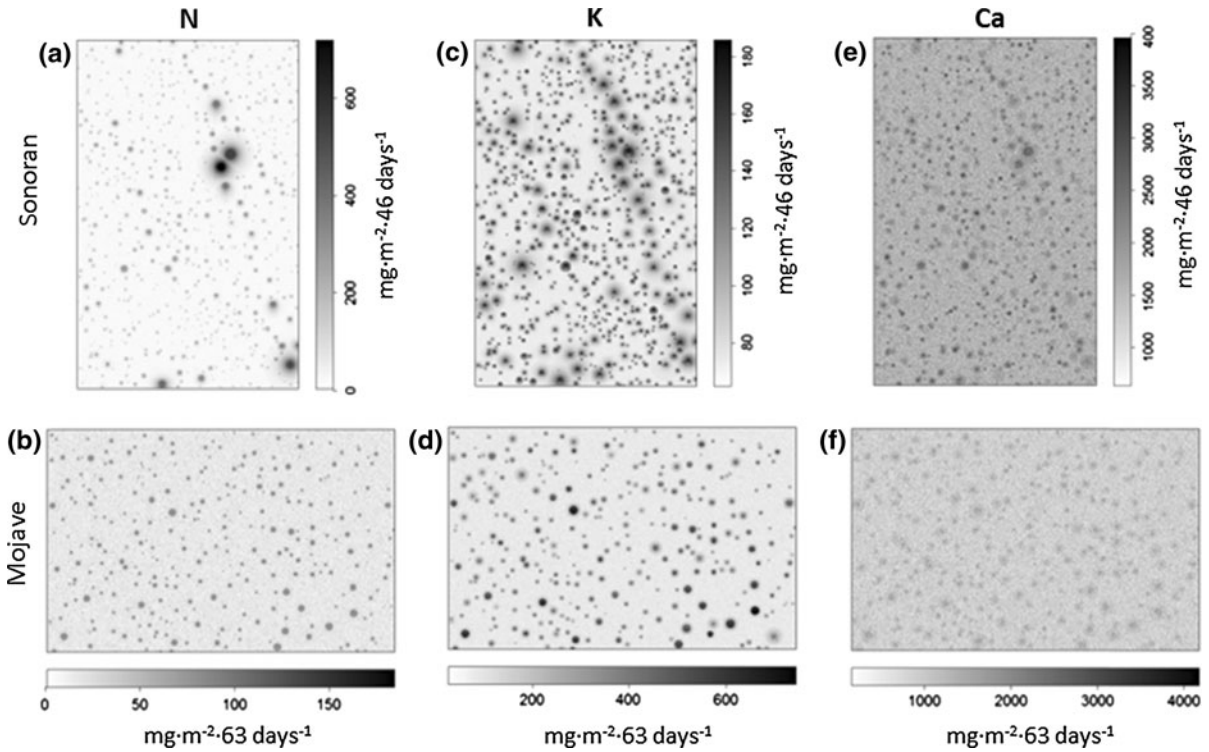

Fig. 5 "Hotspot" maps for N, K and Ca in each desert showing the best models (Table 1) applied to all shrubs in the macroplot

trend model provided the best fit to the Mg data, indicating a slight trend with higher values on the east side of the macroplot (Table 1). Overall, neither Mg model (Mojave or Sonora) provided a very good fit to the validation data (Table 2).

Discussion

We found strong evidence for the presence of fertility islands for N and K, and slightly weaker evidence for Ca. In contrast, concentrations of P and Mg were only

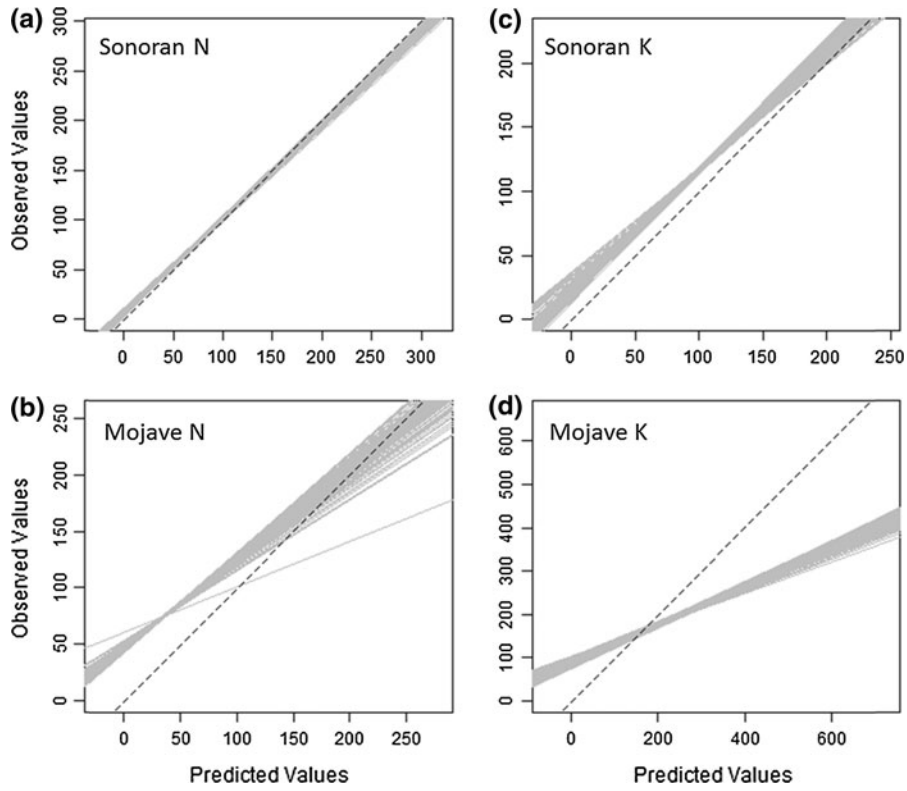

Fig. 6 Regression lines (*gray*) for 100 simulations of best models for N and K (shown in Table 1) for both deserts. *Dotted line* shows Observed = Predicted, corresponding to perfect prediction of validation data (collected in 2012) by values estimated from realizations of models fitted to 2011 data

slightly influenced by shrub position in the Sonora, and not at all in the Mojave. The presence of two growing seasons in the Sonoran Desert may contribute to stronger effects of shrubs, and annual plants, on the distribution of nutrients. Many other studies have found the effect of fertility islands to be multivariate, involving several nutrients (e.g. Charley and West 1975; Schlesinger et al. 1996; Butterfield and Briggs 2009; Li et al. 2011). In our case, negative exponential models were successful in predicting our validation data for nutrients responding strongly to shrubs (Table 1). When the successful models are applied in predicting two-dimensional patterns of distribution, the nutrients form "hotspots" that clearly correspond with shrub canopies (Fig. 5). Since shrub size, measured as area, was a significant predictor of nutrient distribution in many of our models, it may be possible to use remote sensing or aerial imagery to record the position and sizes of shrubs, and then to apply these models to create nutrient maps over a wide area. This is feasible for *Larrea* in desert ecosystems, where shrubs are spaced out and contrast well with the substrate, allowing for easy demarcation from remote imagery (Mudrak 2013). A similar approach is likely feasible in other ecosystems with similar properties that can be remotely sensed.

The ability to predict nutrient concentrations from one year to the next depends on the temporal consistency of the fertility island effect. Researchers have shown that the presence of fertility islands is consistent, but the magnitude can vary monthly (Schade and Hobbie 2005; Wilson and Thompson 2005). For three of the four cases where there was a strong relationship between nutrient concentration and distance from shrub (N in the Sonora and K in both deserts), we had good success in predicting nutrient concentrations in the following year. The precise prediction of N in the Sonora (Fig. 6a) was particularly impressive given the variation in water availability between years. Our models for K in the Sonora were less exact, and consistently underestimated concentrations in the validation data (Fig. 6b). However successful prediction of the spatial pattern of relative nutrient values is still possible when accounting for the variability in magnitude observed between years.

Despite a strong apparent effect of *Larrea* on N in the Mojave (Fig. 4a), our best model could not accurately predict N concentrations. We assessed

other candidate models (not discussed here) incorporating canopy size, but this decreased predictive ability. In our Mojave macroplot, N concentrations were much higher in 2012 than in 2011 and did not seem to follow a negative exponential curve. This difference could be due to greater rainfall during 2012 (1 mm rainfall + 12.5 mm supplemented) as compared to 2011 (7 mm rainfall), which would result in subsequently greater soil moisture. Nitrogen availability is sensitive to water pulses in arid ecosystems (Austin et al. 2004) and net nitrification is higher in wet than in dry desert soils (Esque et al. 2010). Supplemental rainfall may also have created unnatural water potential gradients in the soil, but the greater difference in N concentrations between years, compared to K concentrations, suggests that supplemental rainfall had a greater effect on biological controls of nutrient availability (i.e. microbial activity) than on physical processes (i.e. nutrient diffusion). Successful prediction of N concentrations in the Sonoran Desert may be related to a smaller proportional difference in rainfall between study years (18 % lower in 2012) compared to the Mojave (48 % higher in 2012).

Another reason that our models of N concentrations in the Mojave Desert were less successful could be the presence of the co-dominant shrub *Ambrosia dumosa,* which can also form fertility islands (e.g. Holzapfel and Mahall 1999). We chose to sample shrubs of various sizes of a single species rather than sampling multiple species, as a first step in developing our approach. Butterfield and Briggs (2009) compared fertility islands beneath different species, and while they found interspecific differences, these effect sizes were overshadowed by those of size and growth form. Despite their abundance, *A. dumosa* make up only about one tenth of the canopy volume of *Larrea* in the macroplot, and we were careful to place sampling transects to minimize the influence of the smaller species.

Several of our models contained a significant directional component to the nutrient island effect. For example, our Sonoran models indicate that N concentrations on the north side of *Larrea* were lower and had a faster rate of decay to background levels as a function of distance from the shrub. We found no effect of direction on N in our Mojave site, contradicting findings by Brooks (1998). Our models found that K concentrations were higher under the north side of *Larrea* in the Sonora, but lower in the Mojave (Table 1). Some of the differences in directional effects in the Mojave and Sonoran sites could be due to physical factors, such as local wind and water movement patterns, which affect litter distribution and microbial biomass (Collins et al. 2008). For instance, mesquite litterfall in desert grasslands has been found to be asymmetric—higher on the north and east sides of the stem—due to prevailing winds (Wilson and Thompson 2005). Furthermore, topography differed between our sites; the Sonoran site was flat, while the Mojave site was on a southeast-facing slope. Thus, downslope water flow in the Mojave site could have moved litter from under shrubs, and perhaps more so from the north side.

In addition to directional effects, *Larrea* canopy size was an important predictor of N concentrations in the Sonora and of K concentrations in both deserts. Few studies have explicitly considered perennial canopy size when quantifying fertility islands. Butterfield and Briggs (2009) found species with larger canopies created larger fertility islands, but didn't consider the effects of size within species. *Larrea* litterfall is likely related to canopy size, similar to other arid species (Wilson and Thompson 2005), and could contribute to soil N and K concentrations in our study sites.

What is most interesting about the impact of shrub location and size on the distribution of nutrients is the potential cascading effects within the plant community. Accumulation of nutrients under *Larrea* canopies likely contributes to differences in the abundance and/or biomass of desert annuals under shrubs as compared to interspaces (e.g. Forseth et al. 2001; Brooks 2003; Esque et al. 2010; Schafer et al. 2012). The multivariate nature of fertility island effects we have shown here may have important consequences for the spatial distribution of desert annuals. The relationships between shrub location and size, nutrient distributions, and the distribution of native and exotic annual plants is of key concern because the spread of non-natives in these desert systems has the potential to facilitate fire and alter natural fire regimes (e.g. D'Antonio and Vitousek 1992; Brooks and Matchett 2006). Understanding how non-natives may spread in response to fertility island effects can help inform management decisions aimed at mitigating fire risk.

The techniques developed here can be used to characterize a range of systems where sessile ecosystem engineers play an important role in creating

biogeochemical heterogeneity and structuring plant communities (Rietkerk et al. 2004; Gutierrez and Jones 2006). When successful, these models can be used to characterize two-dimensional patterns of resource distribution using only a small number of well-placed samples. Thus, without increasing sampling effort, these models can greatly increase understanding of spatial patterns of resource availability.

Acknowledgments This study was funded by the Department of Defense's Strategic Environmental Research and Development Program (SERDP) Project RC-1721, Holzapfel & Moloney. Carolyn Haines, Marjolein Schat, Hadas Parag, David Housman, Alex Misiura, Ruth Sparks, Teresa Walker, and Richard Whittle provided logistical support and help in the field. Dennis Lock of the Iowa State University Statistics Consulting Services provided guidance on fitting the non-linear models. AFR is supported by Becas Chile-CONICYT, Ministry of Education, Chile.

References

Abella SR, Craig DJ, Chiquoine LP, Prengaman KA, Schmid SM, Embrey TM (2011) Relationships of native desert plants with Red Brome (*Bromus rubens*): toward identifying invasion-reducing species. Invasive Plant Sci Manag 4(1):115–124

Amoroso L, Miller DM (2006) NTC_Soils. Surficial geologic map of arid Southwest USA. U. S. Geological Survey, Washington, DC

Austin AT, Yahdjian L, Stark JM, Belnap J, Porporato A, Norton U, Ravetta DA, Schaeffer SM (2004) Water pulses and biogeochemical cycles in arid and semiarid ecosystems. Oecologia 141(2):221–235

Baddeley A, Turner R (2005) Spatstat: an R package for analyzing spatial point patterns. J Stat Softw 12(6):1–42

Berger U, Hildenbrandt H (2000) A new approach to spatially explicit modelling of forest dynamics: spacing, ageing and neighbourhood competition of mangrove trees. Ecol Model 132(3):287–302

Bertness MD, Callaway R (1994) Positive interactions in communities. Trends Ecol Evol 9(5):191–193

Brooks ML (1998) Ecology of a biological invasion: alien annual plants in the Mojave Desert. University of California Riverside

Brooks ML (2003) Effects of increased soil nitrogen on the dominance of alien annual plants in the Mojave Desert. J Appl Ecol 40(2):344–353

Brooks ML, Matchett JR (2006) Spatial and temporal patterns of wildfires in the Mojave Desert, 1980–2004. J Arid Environ 67:148–164

Burnham KP, Anderson DR (2004) Multimodel inference—understanding AIC and BIC in model selection. Sociol Methods Res 33(2):261–304

Butterfield BJ, Briggs JM (2009) Patch dynamics of soil biotic feedbacks in the Sonoran Desert. J Arid Environ 73(1):96–102

Charley JL, West NE (1975) Plant-induced soil chemical patterns in some shrub-dominated semi-desert ecosystems of Utah. J Ecol 63(3):945–963

Charley JL, West NE (1977) Micro-patterns of nitrogen mineralization activity in soils of some shrub-dominated semi-desert ecosystems of Utah. Soil Biol Biochem 9(5):357–365

Collins SL, Sinsabaugh RL, Crenshaw C, Green LE, Porras-Alfaro A, Stursova M, Zeglin LH (2008) Pulse dynamics and microbial processes in aridland ecosystems. J Ecol 96(3):413–420

D'Antonio CM, Vitousek PM (1992) Biological invasions by exotic grasses, the grass fire cycle, and global change. Annu Rev Ecol Syst 23:63–87

DeSoyza AG, Whitford WG, MartinezMeza E, VanZee JW (1997) Variation in creosotebush (*Larrea tridentata*) canopy morphology in relation to habitat, soil fertility and associated annual plant communities. Am Midl Nat 137(1):13–26

Drohan PJ, Merkler DJ, Buck BJ (2005) Suitability of the plant root simulator probe for use in the Mojave Desert. Soil Sci Soc Am J 69(5):1482–1491

Esque TC, Kaye JP, Eckert SE, DeFalco LA, Tracy CR (2010) Short-term soil inorganic N pulse after experimental fire alters invasive and native annual plant production in a Mojave Desert shrubland. Oecologia 164(1):253–263

Ewing SA, Southard RJ, Macalady JL, Hartshorn AS, Johnson MJ (2007) Soil microbial fingerprints, carbon, and nitrogen in a Mojave Desert creosote-bush ecosystem. Soil Sci Soc Am J 71(2):469–475

Forseth IN, Wait DA, Casper BB (2001) Shading by shrubs in a desert system reduces the physiological and demographic performance of an associated herbaceous perennial. J Ecol 89(4):670–680

Garcia-Moya E, McKell CM (1970) Contribution of shrubs to nitrogen economy of a desert-wash plant community. Ecology 51(1):81–88

Gutierrez JL, Jones CG (2006) Physical ecosystem engineers as agents of biogeochemical heterogeneity. Bioscience 56(3):227–236

Holzapfel C, Mahall BE (1999) Bidirectional facilitation and interference between shrubs and annuals in the Mojave Desert. Ecology 80(5):1747–1761

Jackson RB, Caldwell MM (1993) Geostatistical patterns of soil heterogeneity around individual perennial plants. J Ecol 81(4):683–692

Jones CG, Lawton JH, Shachak M (1994) Organisms as ecosystem engineers. Oikos 69(3):373–386

Li CJ, Li Y, Ma JA (2011) Spatial heterogeneity of soil chemical properties at fine scales induced by *Haloxylon ammodendron* (*Chenopodiaceae*) plants in a sandy desert. Ecol Res 26(2):385–394

Marion GM, Verburg PSJ, Stevenson B, Arnone JA (2008) Soluble element distributions in a Mojave desert soil. Soil Sci Soc Am J 72(6):1815–1823

McAuliffe JR, Hamerlynck EP, Eppes MC (2007) Landscape dynamics fostering the development and persistence of long-lived Creosotebush (*Larrea tridentata*) clones in the Mojave Desert. J Arid Environ 69(1):96–126

Mudrak E (2013) Using high resolution aerial imagery to determine shrub location & size in creosote flats of the

Sonoran & Mojave Deserts. doi:10.6084/m9.figshare.783022

Muller CH (1953) The association of desert annuals with shrubs. Am J Bot 40(2):53–60

Natural Resources Conservation Service (2005) Soil survey staff, U.S. Department of Agriculture. Soil Survey Geographic (SSURGO) database for Luke Air Force Range, Arizona, Parts of Maricopa, Pima and Yuma Counties. http://soildatamart.nrcs.usda.gov. Accessed 29 Nov 2010

Pinheiro J, Bates D, DebRoy S, Sarkar D, R Development Core Team (2011) nlme: linear and nonlinear mixed effects models. R package version 3.1-102

Qi YC, Dong YS, Jin Z, Peng Q, Xiao SS, He YT (2010) Spatial heterogeneity of soil nutrients and respiration in the desertified grasslands of Inner Mongolia, China. Pedosphere 20(5):655–665

Qian P, Schoenau JJ, Huang WZ (1992) Use of ion-exchange membranes in routine soil testing. Commun Soil Sci Plant Anal 23(15–16):1791–1804

Ribeiro PJ, Diggle PJ (2001) geoR: a package for geostatistical analysis. R-NEWS 1(2): 15–18

Rietkerk M, Dekker SC, de Ruiter PC, van de Koppel J (2004) Self-organized patchiness and catastrophic shifts in ecosystems. Science 305(5692):1926–1929

Ritz C, Streibig JC (2008) Nonlinear Regression with R. Springer Science + Business Media, LLC, New York

Schade JD, Hobbie SE (2005) Spatial and temporal variation in islands of fertility in the Sonoran Desert. Biogeochemistry 73(3):541–553

Schafer JL, Mudrak EL, Haines CE, Parag HA, Moloney KA, Holzapfel C (2012) The association of native and non-native annual plants with *Larrea tridentata* (creosote bush) in the Mojave and Sonoran Deserts. J Arid Environ 87:129–135

Schenk HJ, Mahall BE (2002) Positive and negative plant interactions contribute to a north–south-patterned association between two desert shrub species. Oecologia 132(3):402–410

Schlesinger WH, Raikes JA, Hartley AE, Cross AE (1996) On the spatial pattern of soil nutrients in desert ecosystems. Ecology 77(2):364–374

R Development Core Team (2012) R: a language and environment for statistical computing. R Foundation for Statistical Computing, Vienna. http://www.R-project.org

Western Regional Climate Center (2012) Cooperative climatological data summaries. http://www.wrcc.dri.edu/climatedata/climsum/. Accessed 22 Aug 2012

Whitford WG, Martinez-Meza E, de Soyza A (1996) Morphological variation in Creosotebush, *Larrea tridentata*: effects on ecosystem properties. In: Barrow JR, Durant E, Sosebee RE, Tausch RJ (eds) Proceedings of symposium on shrubland ecosystem dynamics in a changing climate, May 23–25, 1995, Las Cruces, NM. General Technical Report INT-GTR 338. U.S. Department of Agriculture, Forest Service, Intermountain Research Station, Ogden, UT

Whitford WG, Anderson J, Rice PM (1997) Stemflow contribution to the 'fertile island' effect in creosotebush, *Larrea tridentata*. J Arid Environ 35(3):451–457

Wilson TB, Thompson TL (2005) Soil nutrient distributions of mesquite-dominated desert grasslands: changes in time and space. Geoderma 126(3–4):301–315

Wright JP, Jones CG (2006) The concept of organisms as ecosystem engineers ten years on: progress, limitations, and challenges. Bioscience 56(3):203–209